NAVAL POSTGRADUATE SCHOOL

MONTEREY, CALIFORNIA

THESIS

ANALYSIS OF BROADBAND METAMATERIAL SHIELDING FOR COUNTER-DIRECTED ENERGY WEAPONS

by

Chester H. Hewitt III

June 2017

Thesis Advisor: Dragoslav Grbovic
Second Reader: James H. Luscombe

Approved for public release. Distribution is unlimited.

THIS PAGE INTENTIONALLY LEFT BLANK

REPORT DOCUMENTATION PAGE			Form Approved OMB No. 0704-0188
Public reporting burden for this collection of information is estimated to average 1 hour per response, including the time for reviewing instruction, searching existing data sources, gathering and maintaining the data needed, and completing and reviewing the collection of information. Send comments regarding this burden estimate or any other aspect of this collection of information, including suggestions for reducing this burden, to Washington headquarters Services, Directorate for Information Operations and Reports, 1215 Jefferson Davis Highway, Suite 1204, Arlington, VA 22202-4302, and to the Office of Management and Budget, Paperwork Reduction Project (0704-0188) Washington, DC 20503.			
1. AGENCY USE ONLY ***(Leave blank)***	**2. REPORT DATE** June 2017	**3. REPORT TYPE AND DATES COVERED** Master's thesis	
4. TITLE AND SUBTITLE ANALYSIS OF BROADBAND METAMATERIAL SHIELDING FOR COUNTER-DIRECTED ENERGY WEAPONS		**5. FUNDING NUMBERS**	
6. AUTHOR(S) Chester H. Hewitt III			
7. PERFORMING ORGANIZATION NAME(S) AND ADDRESS(ES) Naval Postgraduate School Monterey, CA 93943-5000		**8. PERFORMING ORGANIZATION REPORT NUMBER**	
9. SPONSORING /MONITORING AGENCY NAME(S) AND ADDRESS(ES) Office of Naval Research 875 N Randolph St, Arlington, VA 22217		**10. SPONSORING / MONITORING AGENCY REPORT NUMBER** N0001416WX01128	
11. SUPPLEMENTARY NOTES The views expressed in this thesis are those of the author and do not reflect the official policy or position of the Department of Defense or the U.S. Government. IRB number ____N/A____.			
12a. DISTRIBUTION / AVAILABILITY STATEMENT Approved for public release. Distribution is unlimited.		**12b. DISTRIBUTION CODE**	

13. ABSTRACT (maximum 200 words)

Since the dawn of warfare, arms and armor have been locked in a never-ending struggle for dominance. A new development in that struggle is the advent of high-power microwave (HPM) directed-energy weapons (DEWs), which can disrupt electronics remotely with great accuracy without the need to inflict kinetic damage. Given the importance of electronics in modern warfare, the ability to rapidly develop a counter to such weapons will be essential to sustaining military operations. This thesis investigates the use of microwave-absorbent metamaterials for protection against DEWs and proposes a method for the rapid analysis and design of metamaterial structures. The proposed method uses a parameter retrieval algorithm to characterize a complex metamaterial as a simple, homogenized structure. The retrieved parameters can then be applied to a smooth, homogenized layer in a finite element model, which closely approximates the performance of the original metamaterial analyzed. The homogenized layer model requires far less time and effort to simulate than a complex metamaterial unit cell. The retrieved parameters are applicable to simulated scale models as well, thus reducing the need for physical, scale-model prototypes and accelerating the design process to keep pace with rapidly emerging threats.

14. SUBJECT TERMS metamaterials, microwaves, equivalent medium parameters, homogenization, modeling and simulation, parameter retrieval			**15. NUMBER OF PAGES** 51
			16. PRICE CODE
17. SECURITY CLASSIFICATION OF REPORT Unclassified	**18. SECURITY CLASSIFICATION OF THIS PAGE** Unclassified	**19. SECURITY CLASSIFICATION OF ABSTRACT** Unclassified	**20. LIMITATION OF ABSTRACT** UU

NSN 7540-01-280-5500 Standard Form 298 (Rev. 2-89) Prescribed by ANSI Std. 239-18

THIS PAGE INTENTIONALLY LEFT BLANK

Approved for public release. Distribution is unlimited.

ANALYSIS OF BROADBAND METAMATERIAL SHIELDING FOR COUNTER-DIRECTED ENERGY WEAPONS

Chester H. Hewitt III
Lieutenant, United States Navy
B.S., United States Naval Academy, 2009

Submitted in partial fulfillment of the
requirements for the degree of

MASTER OF SCIENCE IN APPLIED PHYSICS

from the

NAVAL POSTGRADUATE SCHOOL
June 2017

Approved by: Dragoslav Grbovic
Thesis Advisor

James H. Luscombe
Second Reader

Kevin B. Smith
Chair, Department of Physics

THIS PAGE INTENTIONALLY LEFT BLANK

ABSTRACT

Since the dawn of warfare, arms and armor have been locked in a never-ending struggle for dominance. A new development in that struggle is the advent of high-power microwave (HPM) directed-energy weapons (DEWs), which can disrupt electronics remotely with great accuracy without the need to inflict kinetic damage. Given the importance of electronics in modern warfare, the ability to rapidly develop a counter to such weapons will be essential to sustaining military operations. This thesis investigates the use of microwave-absorbent metamaterials for protection against DEWs and proposes a method for the rapid analysis and design of metamaterial structures. The proposed method uses a parameter retrieval algorithm to characterize a complex metamaterial as a simple, homogenized structure. The retrieved parameters can then be applied to a smooth, homogenized layer in a finite element model, which closely approximates the performance of the original metamaterial analyzed. The homogenized layer model requires far less time and effort to simulate than a complex metamaterial unit cell. The retrieved parameters are applicable to simulated scale models as well, thus reducing the need for physical, scale-model prototypes and accelerating the design process to keep pace with rapidly emerging threats.

THIS PAGE INTENTIONALLY LEFT BLANK

TABLE OF CONTENTS

THIS PAGE INTENTIONALLY LEFT BLANK

LIST OF FIGURES

ACKNOWLEDGMENTS

This work was sponsored by the Office of Naval Research (ONR), under grant (or contract) number N0001416WX01128.

I would also like to thank Dr. Jesus Gil Gil and Dr. Brian Meyerhoffer at the Naval Research Laboratory.

THIS PAGE INTENTIONALLY LEFT BLANK

I. INTRODUCTION

Electromagnetic metamaterials are being developed and employed in a variety of applications such as sensing [1], imaging and optics [2], and signature reduction and cloaking [3]. One application of particular interest to the military is the need for electromagnetic protection to defend battlefield electronics against high-power microwave (HPM) directed-energy weapons (DEWs) currently under development worldwide [4]. HPM DEWs are a popular branch of DEW research, as microwaves propagate in the atmosphere more readily than high-energy lasers or particle beams, and HPM DEWs offer a viable non-kinetic option when collateral damage is to be avoided or a kinetic option is unavailable. However, prior research has demonstrated that properly constructed electromagnetic metamaterials are able to prevent microwave transmission by redirecting the incident wave into either absorption or reflection [4]. Such metamaterial shields are typically designed as composite structures consisting of patterned, conductive elements integrated with dielectric materials and arrayed in a manner that generates a desired, predictable spectral response [4]. An example of a metamaterial structure can be seen in Figure 1. Depending on the application, such metamaterials can become structurally complex, which makes them very difficult to model and simulate, particularly across a large frequency domain.

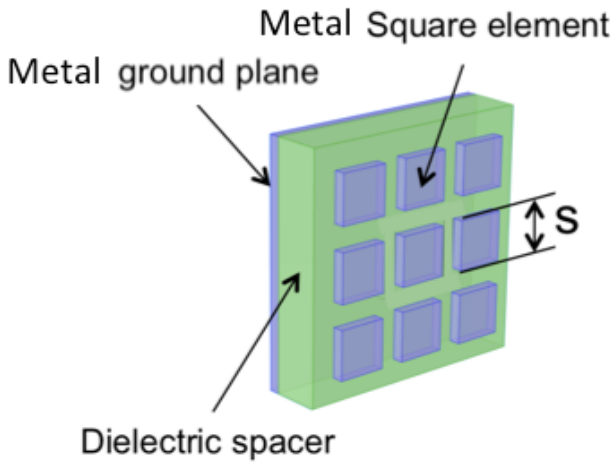

Figure 1. Sample Metamaterial Surface Structure.
Source: [5].

The purpose of this thesis is to present a method for retrieving equivalent medium parameters from a metamaterial structure, and then use those parameters in a homogenized finite element model in order to streamline simulation and design of macroscopic-scale objects made of metamaterials. The method proposed in this paper uses scattering data from either a simulation of a precise metamaterial structure or an experimental measurement of an actual metamaterial sample. With that data, it develops characteristic reflection and transmission spectra for the metamaterial. The characteristic coefficients are used in a system of equations to calculate the frequency-dependent properties for an equivalent homogeneous material, that would respond to the electromagnetic incident radiation equivalently to the sampled metamaterials. The derived properties can then be applied to a homogeneous layer in a finite element model. The result is a simplified computer model, which closely mimics the performance of the original, structurally complex, metamaterial sample, but which can be readily modified in scale and geometry without additional computational burden. A designer would thus be able to rapidly conduct simulated scale-model testing of a metamaterial assembly without the need for multiple physical models.

Numerous systems of equations have been developed that consider electromagnetic metamaterials as homogeneous structures parameterized with frequency-dependent material properties such as permittivity and permeability. Such systems typically branch into multiple correct solutions, resulting in ambiguity when attempting to select the correct set of homogenized parameters [6]–[8]. Methods for resolving branch ambiguity usually require a material with a known permittivity and permeability at a known frequency [7]–[9], parameters collected from multiple thicknesses of the material [6], [7], or parameters collected across multiple frequencies [7]. In the case of this method, the initial material properties of the metamaterial were unknown, multiple thicknesses of the material were unavailable, and the simplest metamaterial analyzed was only resonant at a single frequency. The proposed method instead addresses branch ambiguity as the ratio between the effective medium transmission path and effective wavelength in the medium [9]. Although previously proposed systems deal in effective permittivity and permeability for a metamaterial, the finite element models employed for this research also required electrical conductivity in order to successfully predict the scattering parameters, attenuation within the simulated medium and joule heating in response to absorbed radiation. The proposed method presents an expression for estimating effective conductivity from the impedance and the geometry of the metamaterial unit cell. Finally, prior research rarely extrapolated the performance of the retrieved parameters outside the unit cell analyzed [6], [7]. The proposed method retrieves parameters valid for a homogenized scale model as well as a periodic unit cell.

THIS PAGE INTENTIONALLY LEFT BLANK

II. THEORY AND METHOD

A. THEORY AND SYSTEM OF EQUATIONS

In order to model metamaterials as a homogeneous medium, the metamaterial unit cells should ideally have a physical size 10–30 times smaller than the reference wavelength to be absorbed [9]. A periodic structure of such small elements would function as a truly homogeneous medium with frequency-dependent homogenized parameters valid for all incident angles. The metamaterials used for this research do not meet this homogenization criterion, as the metamaterial resonator widths are no more than three times smaller than the absorbed wavelengths in some portions of the spectrum of interest. As a result, the homogenized parameters derived from this research should be considered *equivalent medium* parameters: frequency-dependent parameters that provide a good prediction of scattering characteristics and dissipation within the medium at near-normal angles of incidence

The analytical retrieval method employed is outlined in [6]. The metamaterials' experimental scattering parameters from a sampled spectrum were converted to the corresponding reflection coefficients, r [10]. To simplify annotation throughout the equations, we substitute the frequency-dependent normalized transmission coefficients from the equation:

$$t' = te^{ikd} \tag{1}$$

where $k = \omega/c$ is the wavenumber of the incident radiation and the magnitude t is assumed to be small (in our algorithm, on the order of 10^{-4}). With the reflection and transmission coefficients we calculated impedance as:

$$z = \sqrt{\frac{\left(1-r^2\right)-t'^2}{\left(1+r^2\right)-t'^2}} \tag{2}$$

with r representing the frequency-dependent reflection coefficients. To calculate permittivity and permeability we require the metamaterial effective index of refraction n derived from the equation:

$$cos(nkd) = \frac{1}{2t'}\left[1-\left(r^2 - t'^2\right)\right] \tag{3}$$

where d is the effective metamaterial thickness. In this case we approximated d as an *effective medium depth* equal to twice the metamaterial physical thickness. An area of major difficulty that arises in applying this equation to metamaterials with a solid ground plane is that transmission is near zero, as confirmed by both simulation and experiment (the ground plane in our case is larger than the skin depth for all frequencies of interest), which induces a singularity in the *1/2t'* term of Eq. 3. In order to use Equation 3 to provide equivalent medium parameters, it is necessary to use a transmission term that is negligible but non-zero. From the above equation, the complex components of n are solved as:

$$Im(n) = Im\left(\frac{cos^{-1}\left(\frac{1}{2t'}\left[1-\left(r^2 - t'^2\right)\right]\right)}{kd}\right) \tag{4}$$

$$Re(n) = Re\left(\frac{cos^{-1}\left(\frac{1}{2t'}\left[1-\left(r^2 - t'^2\right)\right]\right)}{kd}\right) + \frac{2\pi m}{kd} \tag{5}$$

For the real component of n, the integer m refers to the propagation branch of the metamaterial and should be approximate to the ratio between the transmission path and the wavelengths length [9]. Since our shortest absorbed wavelength is still over ten times longer than the metamaterial transmission path, we used the initial assumption $m = 0$. However, as noted in [9], a highly absorbent material, with a high index of refraction, can result in an effective medium path length several times longer than the effective medium wavelength, despite the thin physical depth of the sample. Therefore, it is necessary to

ascertain a consistent propagating mode and ensure the effective path length is consistent with the index of refraction. Ultimately, the criteria $m \approx nd/\lambda$ should be satisfied. In terms of deriving homogenized parameters, it is crucial that the metamaterial be described by a single propagating mode [9].

Using n and z, electric permittivity ε and magnetic permeability μ are obtained as:

$$\varepsilon = \frac{n}{z} \tag{6}$$

$$\mu = nz \tag{7}$$

However, completion of the finite element model also requires a frequency-dependent volume conductivity parameter in order to predict the correct scattering parameters, given by:

$$\sigma = \left(\frac{d}{Az} \right) \tag{8}$$

where A is the surface area of the metamaterial unit cell. We chose the reference area to be normal to the Poynting vector of the incident radiation. Conductivity is thus proportional to permittivity through the inverse of impedance. Although others have attempted to apply bulk conductivity to metasurfaces through direct measurement [11], Equation 8 is unique in that it offers an analytic interpretation of conductivity for a homogenized metamaterial.

B. RETRIEVAL ALGORITHM

The equations described in the previous section were implemented as parametric algorithms operating in the spectrum of interest. Frequency-dependent reflection coefficients were derived from S_{11} parameter measurements, imported either from simulated models or from experimental measurements of physical samples taken in an anechoic chamber. To generate the value of transmission required for Equation 1, uniform transmission on the

order of 10^{-4} was assumed at all data points within the bandwidth, given that transmission through the copper ground plane is expected to be negligible. Use of actual insertion loss data would likely improve the overall quality of the model, as any actual transmission, however negligible, is likely frequency dependent. Any remainder, not accounted for by reflection or transmission, was assumed to be resistive attenuation within the metamaterials, as second order scattering can be considered negligible for such structures [12]. Appendix A contains the complete retrieval algorithm coded in MATLAB, and Figure 2 shows a flow chart of the complete retrieval process.

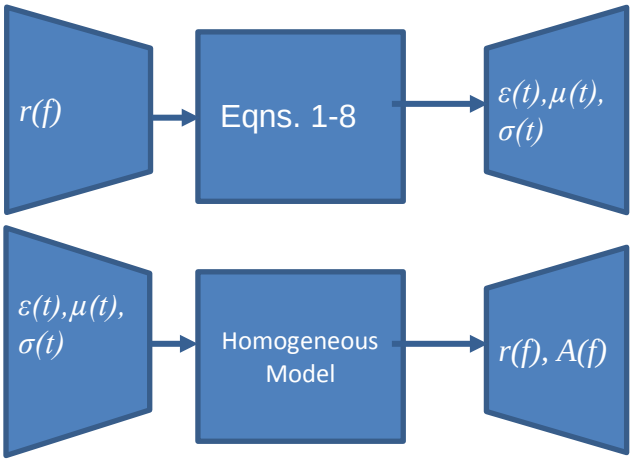

Figure 2. Retrieval Process / Process of Using Retrieved Parameters in the Model.

III. DATA COLLECTION AND ANALYSIS

A. CASE STUDY 1: RETRIEVAL OF PARAMETERS FROM A SIMULATED SINGLE BAND METAMATERIAL STRUCTURE

To verify the retrieval process, simulated frequency dependent reflection data was extracted from a model of a simple, single band, microwave absorbent metamaterial unit cell. The unit cell had length and width of 11 mm and overall physical depth of 146 um. The metamaterial consisted of a ~9 mm wide copper square mounted on dielectric with an index of refraction of ~2.16. As noted in [13] the resonant frequency can be predicted as:

$$f = \left(\frac{c}{2nw} \right) \tag{9}$$

where c is the speed of light, n is the index of refraction for the dielectric, and w is the width of the conductive square. For the single band metamaterial model, the resonant peak was tuned to 7.72 GHz. The retrieval algorithm extracted the equivalent medium parameters from the reflection data, and the equivalent medium parameters were then applied to a simulated homogenized medium with effective depth matching the effective depth used in the algorithm. Figure 3 shows the finite element model for equivalent homogeneous material, as well as a depiction of the electric field attenuating within the model. For branch 1, the index of refraction at resonant frequency was found to be 134. When index of refraction was multiplied by the effective medium depth 292 um, the product was 39 mm, approximate to the 39 mm wavelength at 7.72 GHz. Thus, the criteria $m \approx nd/\lambda \approx 1$ from [9] was satisfied for branch 1.

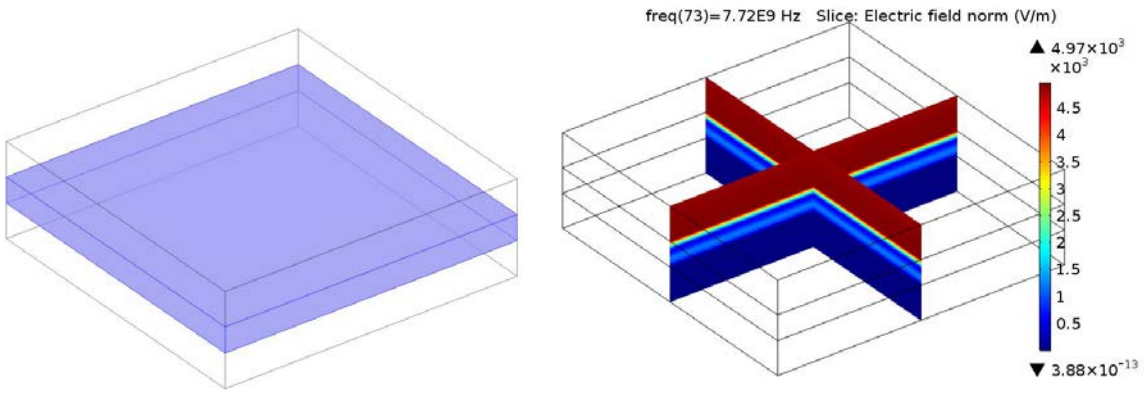

(a) (b)

(a) Shows the homogenized volume that the equivalent medium parameters were applied to.

(b) Shows the simulated electric field attenuating within the homogenized medium.

Figure 3. Homogenized Unit Cell. (a) Initial Setup. (b) Simulated Electric Field.

Figure 4 compares the simulated reflection coefficients for branch 1 compared to those predicted by the COMSOL homogenized model. Since it is common to obtain the absorption spectrum in metamaterial like these as $A = 1 - R$ [11] through the assumption that whatever was not reflected was dissipated as heat loss, this method was tested against the absorption obtained from the model by volume integration of Joule heating losses. Through volume integration of Joule heating, COMSOL was also able to predict resistive losses correlated to the anticipated absorption within the medium. Figure 5 compares the simulated resistive losses with the predicted resistive losses for the single band model.

Although the COMSOL homogenized unit cell represents a sound approximation of the actual metamaterials used, the ultimate goal is to be able to scale the COMSOL homogenized model to any size and shape and still have a good approximation for overall performance. Therefore, the original unit cell model's surface area was scaled up from 11 mm width to 22 cm width to approximate the actual 20 by 20 unit cell plates to be used for experimental S_{11} measurements. Aside from length and width, all other properties were left

unperturbed. Figure 4 and Figure 5 also show the output from the simulated scale model, demonstrating a very close agreement between the scale model, the unit cell model, and the original input data.

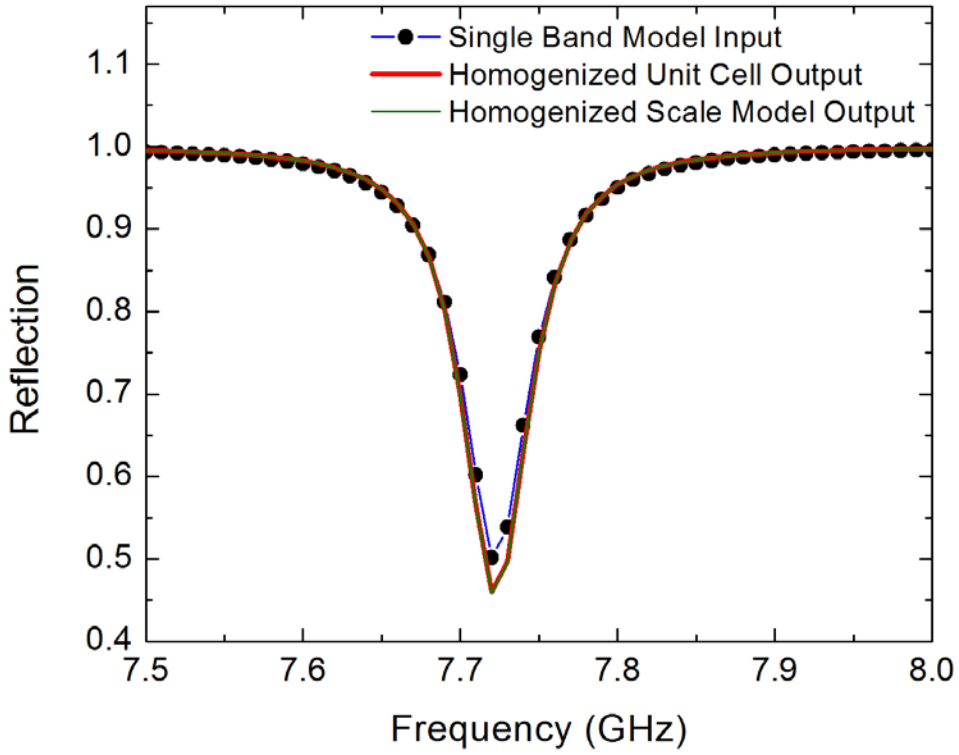

Comparison of output from single band model and equivalent homogeneous medium models. The black points and fitted blue line indicate the original reflection data points input to the retrieval algorithm. The red line indicates the reflection output from a homogenized unit cell using the retrieved equivalent medium parameters. The green line indicates the reflection output from a homogenized scale model using the same retrieved equivalent medium parameters.

Figure 4. Reflection Comparison for Simulated Single Band Metamaterial

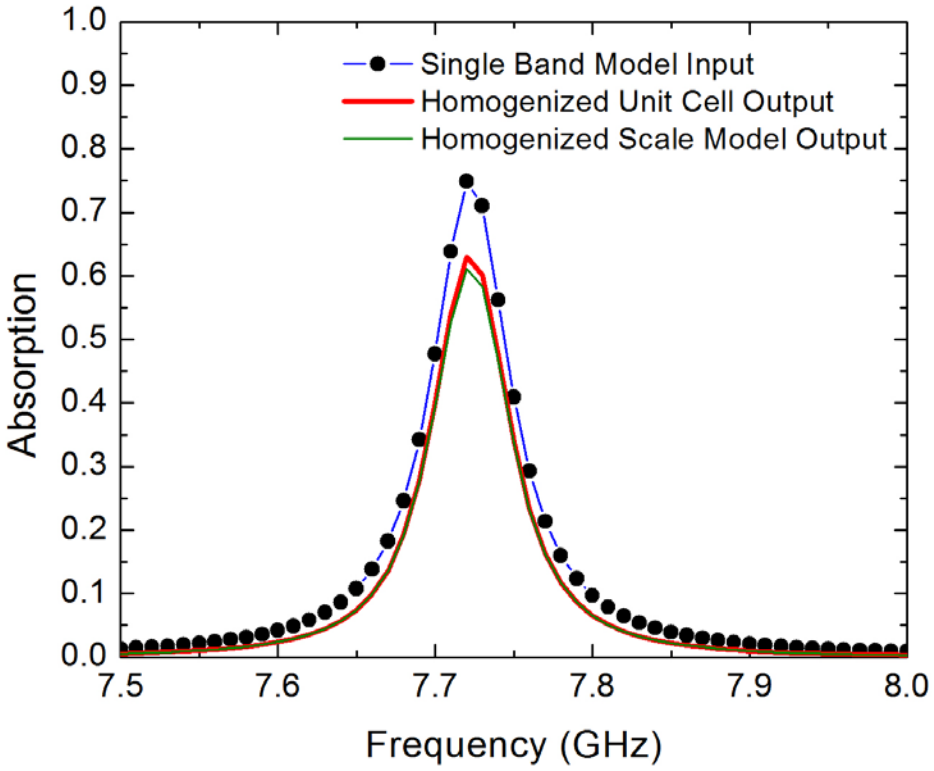

Comparison of output from single band model and equivalent homogeneous medium models. The black points and fitted blue line indicate the absorption predicted by the original simulated model. The red line indicates the absorption predicted by a homogenized unit cell using the retrieved equivalent medium parameters. The green line indicates the absorption predicted by a homogenized scale model using the same retrieved equivalent medium parameters.

Figure 5. Absorption Comparison for Simulated Single Band Metamaterial

B. CASE STUDY 2: RETRIEVAL OF PARAMETERS FROM A SIMULATED BROADBAND METAMATERIAL

To further validate the retrieval algorithm, the same procedure was followed with a simulated broadband structure consisting of six laminated resonator layers (depicted in Figure 6) to see if the algorithm could homogenize a metamaterial with multiple features over a wide bandwidth. The broadband structure was developed to model a material sample to be used for experimental analysis (discussed later in Section C). The broadband model unit cell has a length and width of 11 mm and depth of 922 um.

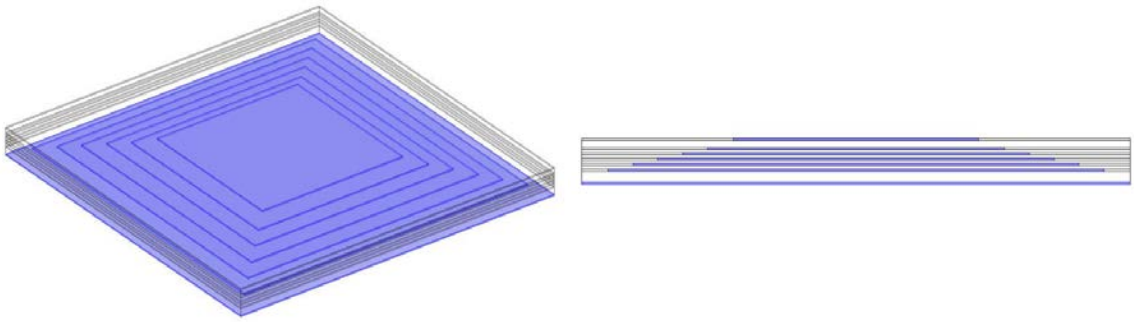

(a) (b)

Conductive layers highlighted

Figure 6. Broadband Model Illustration. (a) 3D View. (b) Profile View.

The retrieval algorithm was again used to process simulated reflection data into frequency dependent equivalent medium parameters. For branch 4, the index of refraction at the resonant frequency 7.54 GHz was found to be 87. When index of refraction was multiplied by the effective medium depth 1.844 mm, the product was 160 mm, approximate to 4 times the 40 mm wavelength at 7.54 GHz. The outcome $m \approx nd/\lambda \approx 4$ remained consistent at the resonant points in the spectrum.

As with the single band case, the equivalent medium parameters were applied to both simulated unit cell and scale homogenized models, and again good agreement was achieved between the input data and the corresponding simulations. Figure 7 shows the comparisons for reflection between the original model, the homogenized unit cell, and the homogenized scale model. Figure 8 shows the comparisons for resistive losses between the original model, the homogenized unit cell, and the homogenized scale model.

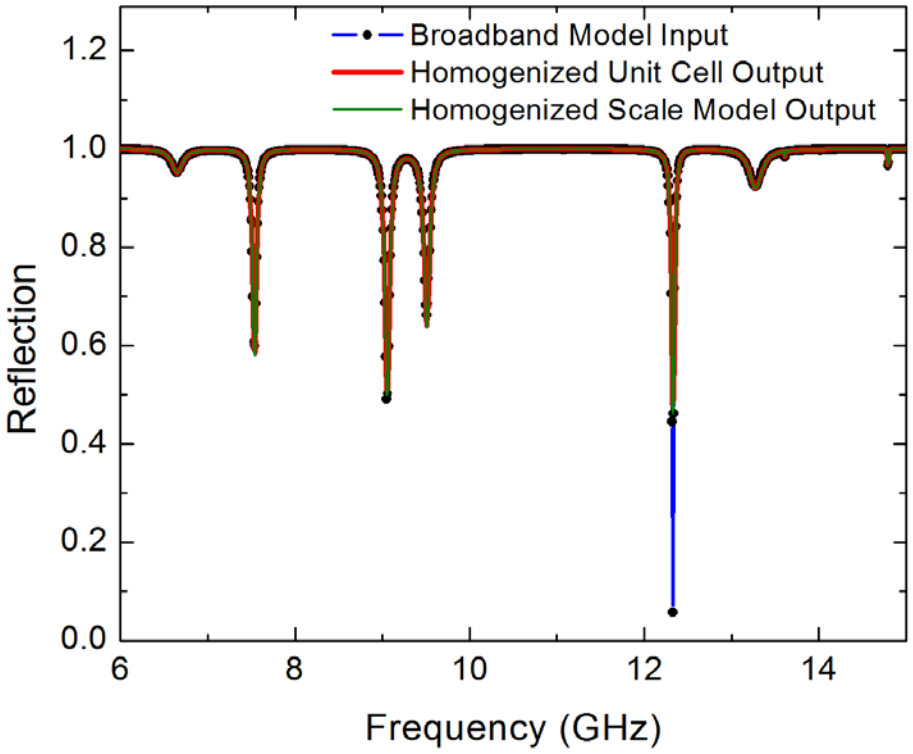

Comparison of output from broadband model and equivalent homogeneous medium models. The black points and fitted blue line indicate the original reflection data points input to the retrieval algorithm. The red line indicates the reflection output from a homogenized unit cell using the retrieved equivalent medium parameters. The green line indicates the reflection output from a homogenized scale model using the same retrieved equivalent medium parameters. Note the six resonant points, corresponding to the six conductive layers, all of which are captured by the equivalent medium parameters.

Figure 7. Reflection Comparison for Simulated Broadband Metamaterial.

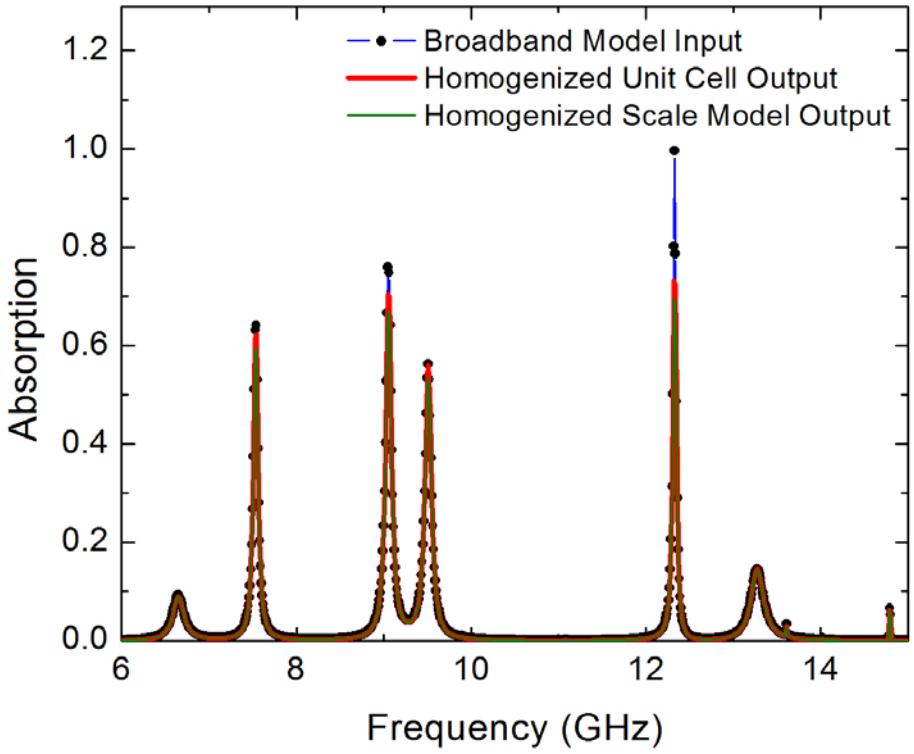

Comparison of output from broadband model and equivalent homogeneous medium models. The black points and fitted blue line indicate the absorption predicted by the original simulated model. The red line indicates the absorption predicted by a homogenized unit cell using the retrieved equivalent medium parameters. The blue line indicates the absorption predicted by a homogenized unit cell using the same retrieved equivalent medium parameters. Note the six resonant points, corresponding to the six conductive layers, all of which are captured by the equivalent medium parameters.

Figure 8. Absorption Comparison for Simulated Broadband Metamaterial.

C. CASE STUDY 3: RETRIEVAL OF PARAMETERS FROM EXPERIMENTAL BROADBAND METAMATERIAL DATA

The metamaterial used for the experimental portion of the study was a microwave-absorbent design, consisting of copper resonator layers of various widths, interspersed with layers of dielectric material (in this case two grades of circuit board fiberglass), anchored on a continuous copper ground plane. Scattering parameters were measured from a plate with a 20 by 20 array of 11 mm unit cells as shown in Figure 9.

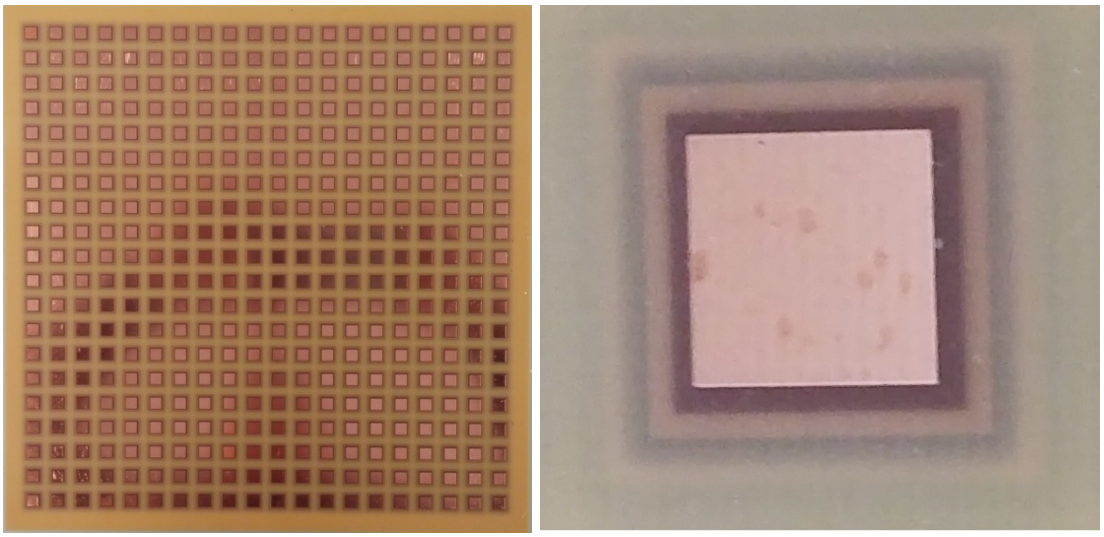

(a) (b)

Figure 9. (a) Photograph of 22cm Metamaterial Test Plate. (b) Close-Up of Unit Cell.

Each unit cell contains six copper resonator layers varying in width between 5 mm and 10 mm stepped in 1 mm increments. Figure 10a and Figure 10b show 3D and profile images taken with the Scanning Electron Microscope (SEM) in Spanagel Hall. For purposes of the homogenized model, each unit cell was assumed to be 11 mm in length and width and 922 um in depth based on an average of samples measured with the SEM. Scattering data for the metamaterial sample was provided by the Naval Research Laboratory, and the experimental setup in the laboratory's anechoic chamber can be seen in Figure 11.

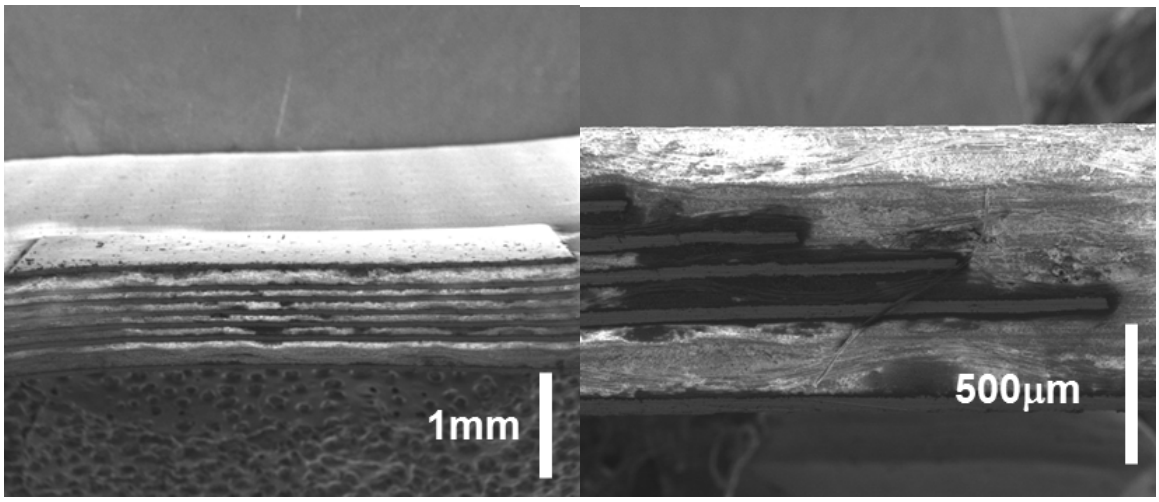

(a) (b)

Figure 10. (a) SEM Wide View of Metamaterial Unit Cell. (b) SEM Profile View of Metamaterial Unit Cell Edge.

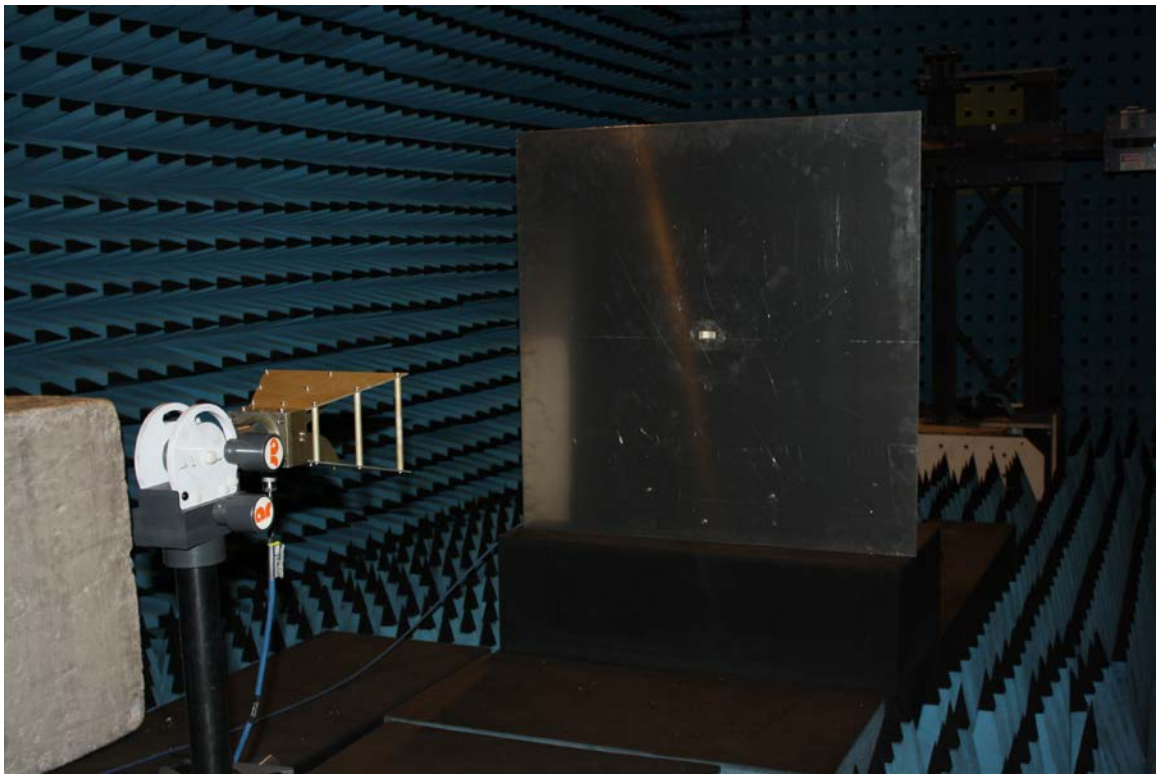

Figure 11. Experimental Setup for Scattering Parameter Measurements. Source: [14].

The retrieval algorithm was applied to the experimental reflection data. Branch 4 was also chosen for the experimental data, and a comparison of the original reflection data and homogenized outputs (unit cell and scale model) can be seen in Figure 12. The associated absorption comparisons can be seen in Figure 13. The models demonstrate good agreement with the experimental data, although there are some discrepancies in amplitude at the points of greatest attenuation in the spectrum. The discrepancies are likely the result of violations of the homogenization criteria at those specific points. While the transmission levels and propagation modes assumed gave valid predictions throughout most of the spectrum, it is entirely possible that the highly absorbent points would be better characterized by different homogenization assumptions. Although the models leave room for further refinements, the homogenized predictions still show generally strong correlation to the measured input data.

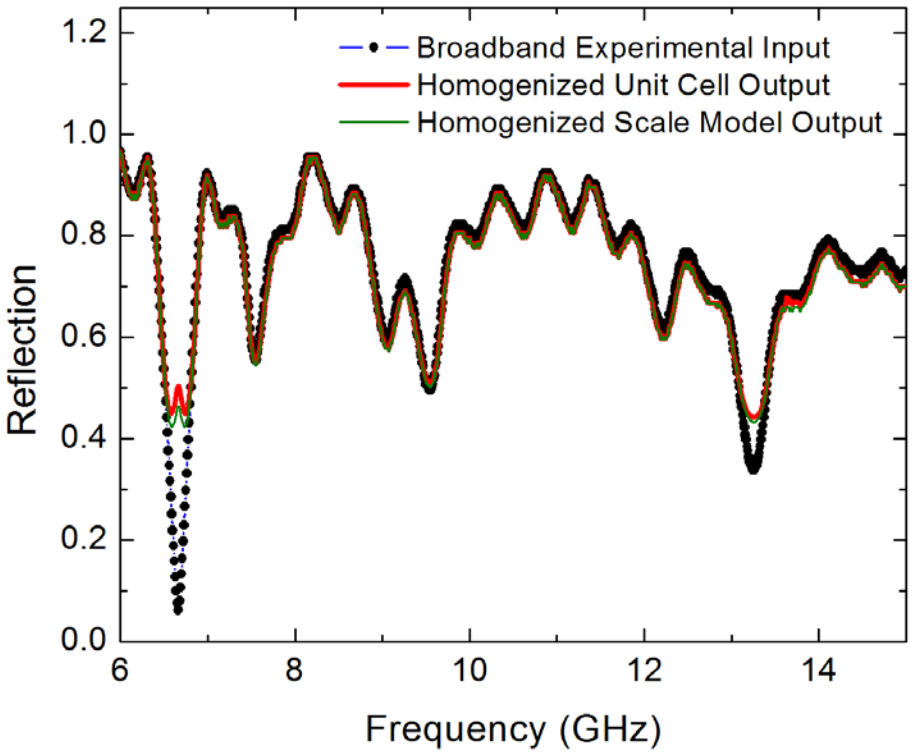

Comparison of output from broadband model and equivalent homogeneous medium models. The black points and fitted blue line indicate the original reflection data points input to the retrieval algorithm. The red line indicates the reflection output from a homogenized unit cell using the retrieved equivalent medium parameters. The green line indicates the reflection output from a homogenized scale model using the same retrieved equivalent medium parameters. The equivalent medium parameters capture not only the six resonant points associated with the six conductive layers, but several other features present in the spectrum.

Figure 12. Reflection Comparison for Experimental Broadband Metamaterial

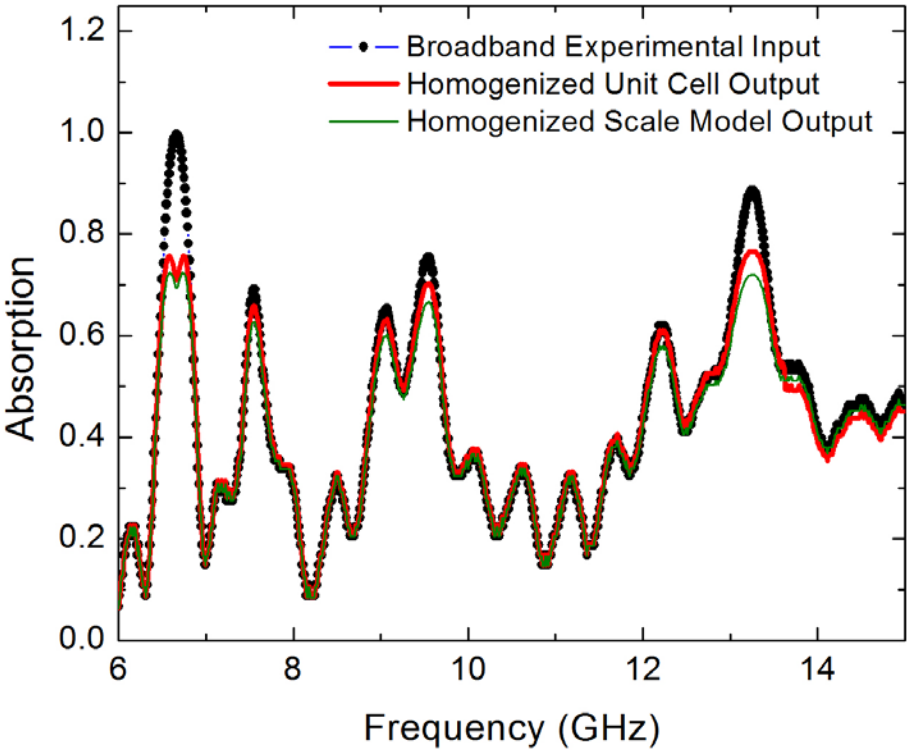

Comparison of output from broadband model and equivalent homogeneous medium models. The black points and fitted blue line indicate the absorption predicted by the original simulated model. The red line indicates the absorption predicted by a homogenized unit cell using the retrieved equivalent medium parameters. The blue line indicates the absorption predicted by a homogenized unit cell using the same retrieved equivalent medium parameters. The equivalent medium parameters capture not only the six resonant points associated with the six conductive layers, but several other features present in the spectrum.

Figure 13. Absorption Comparison for Experimental Broadband Metamaterial

IV. CONCLUSION

A. SUMMARY OF RESULTS

The proposed method uses simulated or experimental scattering data from a structure of unknown parameters and processes the data with a retrieval algorithm that provides equivalent medium parameters for an analogous homogenized structure. The equivalent medium parameters permit rapid modeling of complex structures that are difficult and time-consuming to simulate. The proposed method also verifies the approach from [9] to overcome branch ambiguity, inherent in the optical equations for parameter retrieval. We further augment the model by an expression for effective conductivity, useful for finite element modeling. The equivalent medium parameters derived prove applicable to a scale model of a periodic metamaterial structure, obviating the need to model individual unit cell elements at the macroscopic level. The method facilitates and accelerates simulated scale model testing of complicated metamaterial structures, all based on the data collected from a single representative prototype.

In terms of confronting the threat posed by HPM DEWs, adaptability and speed are of the utmost importance to the procurement of HPM shielding. Because HPM DEWs constitute a wide variety of threats across a vast spectrum, in an ideal situation properly tuned shielding should be made available on demand. A better understanding of metamaterial physics combined with the ability to accurately simulate shielding performance will allow manufacturers to update computer-aided design models accordingly, and enable rapid 3D printing or additive manufacturing of shielding as it is required to counter the weapon system assessed. The more modular and adaptable the shielding, the better it will be at keeping pace with the threat. Such an approach would circumvent several of the bottlenecks associated with the traditional acquisition process and expedite delivery of protection to the warfighter.

B. FUTURE WORK

Although the current version of the algorithm generates good agreement between a unit cell response and a scaled up slab response, further research will investigate whether the algorithm successfully generates equivalent medium parameters for macroscopic objects with alternate geometry, such as a spherical radome. Figure 14 shows a notional example for the size and type of geometry to be investigated.

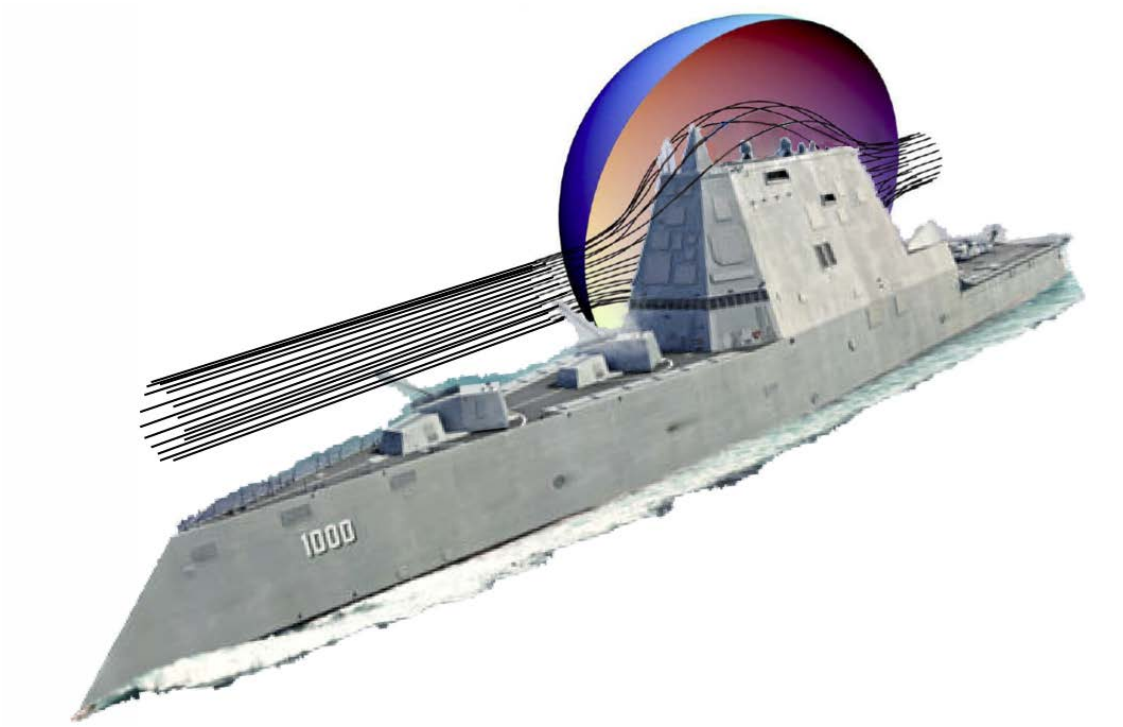

Figure 14. Macroscopic Finite Element Model of Shipboard Protection. Source: [5].

While HPM shielding is useful, the shielding will be even more valuable if it can also function as a passive sensor. As shown in Figure 15, at resonance the electric fields internal to the metamaterial structure are highly localized around the corresponding conducting layer.

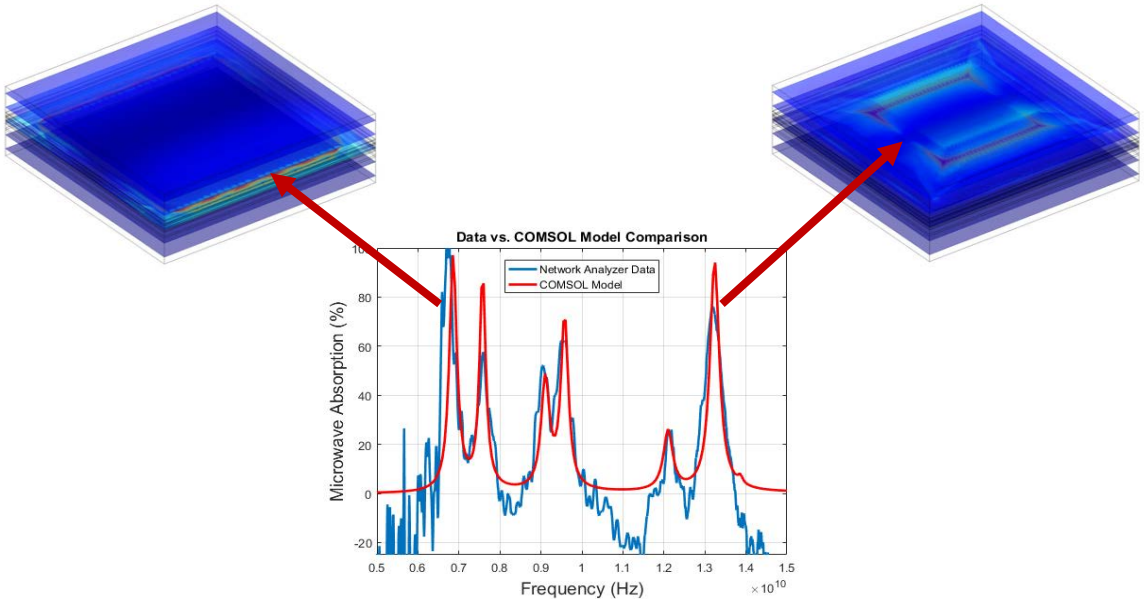

At resonance, electric fields become highly localized around the conductor associated with that frequency response. The model in the top right shows the electric field around the 5 mm conductor plate at 13.3 GHz, correlated to an absorption peak in the spectrum at 13.4 GHz. Likewise, the model in the top left shows a localized field around the 10 mm plate at 6.7 GHz, correlated to the absorption peak at 6.7 GHz.

Figure 15. Localization of Electric Fields Within Broadband Metamaterial

Follow-on research will attempt to exploit these localized electric fields by incorporating field effect transistors between the metamaterial layers. In this way the shielding will provide situational awareness and data on the attacking waveform in addition to protecting the vulnerable equipment underneath. At NPS, such an approach has already been incorporated into terahertz imaging metamaterials, as shown in Figure 16.

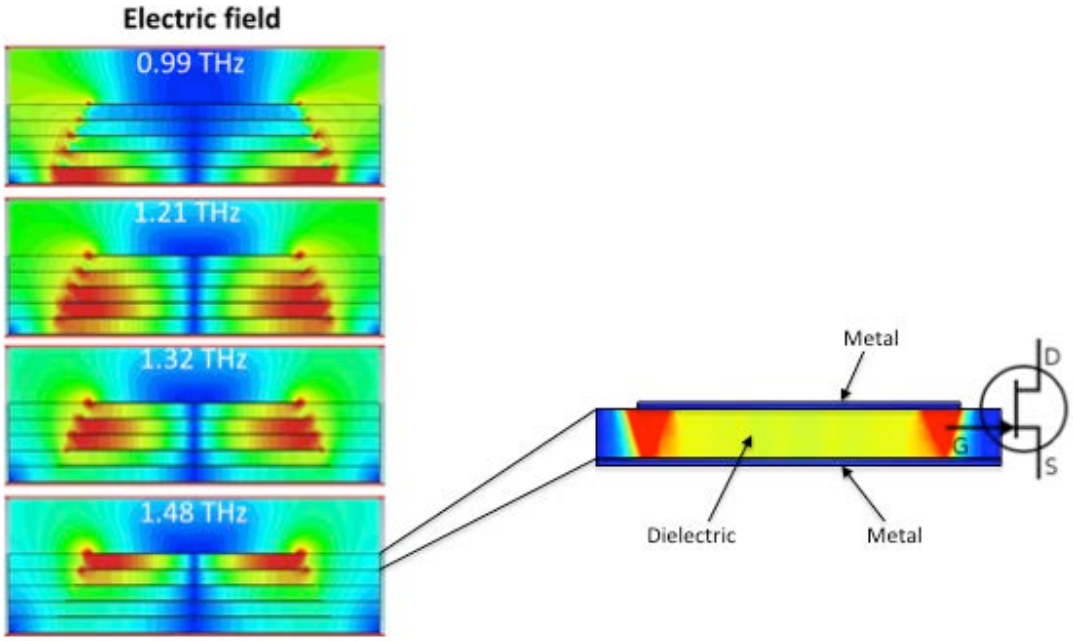

Figure 16. Use of Transistors in Terahertz Metamaterials.
Source: [5].

However, one challenge associated with incorporation of transistors into microwave metamaterials is that test equipment may not be able to generate fields strong enough to be detected by the transistors. Therefore, NPS will be partnering with the HPM segment of the NAVSEA Directed Energy Warfare Office to not only test the performance and resilience of prototype shielding exposed to actual HPM sources, but also to attempt to gather data from a shielding prototype equipped with transistors.

APPENDIX A. RETRIEVAL ALGORITHM FORMULATED IN MATLAB CODE

```
%% Import Relevant Data (Spectrum and Reflection)

%spectrum_model_SEM = csvread('BroadbandModelSEM.csv',5,0,'A6..A326');
%absorb_model_SEM = csvread('BroadbandModelSEM.csv',5,1,'B6..B326');

%{
spectrum_NRL = csvread('front.csv',1,0,'A2..A1702');
S11_front = csvread('front.csv',1,1,'B2..B1702');
S11_plate = csvread('plate.csv',0,1,'B1..B1701');
S11_normalized = S11_front-S11_plate;
absorb_normalized = (1-10.^(S11_normalized./10));
%}

spectrum_NRL = csvread('COMSOL_SEM.csv',5,0,'A6..A906');
r_model = csvread('COMSOL_SEM.csv',5,1,'B6..B906');

%spectrum_NRL = csvread('COMSOL_SEM_simple.csv',5,0,'A6..A56');
%r_model = csvread('COMSOL_SEM_simple.csv',5,1,'B6..B56');

%% Set Retrieval Assumptions

%r_model = 10.^(S11_normalized./20); % generate reflection matrix
%t = 7.25e-4;
t = 7.25e-4; % set transmission levels
c = 299792458; % define light speed (m/s)
k = 2*pi.*spectrum_NRL./c; % generate wavenumber matrix (radians/m)
d = 2*922e-6; % define transmission path lengths (m)
area = (11/1000)^2; % define unit cell area (m^2)
t_prime = t.*exp(i.*k.*d); % generate transmission matrix
m = 4; % select propagation branch
fudge = 1; % just in case you need a fudge factor for something

%% Retrieve Parameters

z = sqrt(((1.+r_model).^2.-t_prime.^2) ./ ((1.-r_model).^2.-
t_prime.^2)); % generate impedance array

%rho = (146e-6).*z;

rho = (area/d).*z; % solve for volume resistivity (Ohm*m)

sigma = 1./rho; % solve for volume conductivity (S/m)

n = acos((1./(2.*t_prime)).*[1.-(r_model.^2.-t_prime.^2)])./(k.*d); %
generate refractive index array

n_i = imag(n); % extract imaginary component of n
```

```
%{
DO NOT USE
Attempted superposition of propagation modes. However, homogenized
material
must be described by a single propagation branch.
for m = 1:3
    n_branch = real(n) + m*2*pi./(k.*d);
    n_rs(m,:) = n_branch;
end

n_r = sum(n_rs);
%}

n_r = real(n) + m*2*pi./(k.*d); % correct real component of n with
propagation branch m.

n_comp = n_r+i*n_i; % integrate corrected real and imaginary n

epsilon = (n_comp)./z; % solve for permittivity

mu = (n_comp).*z; % solve for permeability

%% Write CSV files to be read by COMSOL.
% Make sure COMSOL interpolation extraction matches file extension.

EpR2a = [spectrum_NRL real(epsilon)];
csvwrite('EpR2a.csv',EpR2a);

EpI2a = [spectrum_NRL imag(epsilon)];
csvwrite('EpI2a.csv',EpI2a);

MuR2a = [spectrum_NRL real(mu)];
csvwrite('MuR2a.csv',MuR2a);

MuI2a = [spectrum_NRL imag(mu)];
csvwrite('MuI2a.csv',MuI2a);

SigR2a = [spectrum_NRL real(sigma)];
csvwrite('SigR2a.csv',SigR2a);

SigI2a = [spectrum_NRL imag(sigma)];
csvwrite('SigI2a.csv',SigI2a);

%% Generate plots of relevant parameters

%{
subplot(2,1,1);
plot(spectrum_NRL./1e9,r_model,'k');
grid on;
title('NRL Experimental Data for Metamaterial Absorption');
%legend('Network Analyzer Raw Data','COMSOL Model');
```

```
%xlabel('Frequency (GHz)');
ylabel('Reflection Coefficient');
axis([6 15 0 1]);


subplot(2,1,2);
plot(spectrum_NRL./1e9,real(epsilon),'r');
grid on;
title('Conductivity');
%legend('Network Analyzer Raw Data','COMSOL Model');
%xlabel('Frequency (GHz)');
ylabel('\sigma (S/m)','FontWeight','bold');
axis([6 15 0 1]);
%}

%
subplot(3,1,1);
plot(spectrum_NRL./1e9,abs(epsilon),'r');
grid on;
title('Permittivity');
%legend('Network Analyzer Raw Data','COMSOL Model');
%xlabel('Frequency (GHz)');
ylabel('\epsilon');
axis([6 15 0 100]);

subplot(3,1,2);
plot(spectrum_NRL./1e9,abs(mu),'r');
grid on;
title('Permeability');
%legend('Network Analyzer Raw Data','COMSOL Model');
%xlabel('Frequency (GHz)');
ylabel('\mu','FontWeight','bold');
axis([6 15 0 50000]);

subplot(3,1,3);
plot(spectrum_NRL./1e9,abs(sigma),'r');
grid on;
title('Conductivity');
%legend('Network Analyzer Raw Data','COMSOL Model');
xlabel('Frequency (GHz)');
ylabel('\sigma (S/m)','FontWeight','bold');
axis([6 15 0 1]);
%}
```

THIS PAGE INTENTIONALLY LEFT BLANK

APPENDIX B. ADDITIONAL NOTES ON BRANCH SELECTION

The selection of the propagation branches (described in Equation 5) for each metamaterial was ultimately achieved through a systematic process of trial and error. Beginning with the branch selection $m=0$, the algorithm and homogenized simulation were run several times stepping through the integer branches, until the branch offering the closest match to the input data was ascertained and selected. Although this is not a perfect solution to the branch ambiguity problem, it is very practical compared to other methods investigated for resolving branch ambiguity.

THIS PAGE INTENTIONALLY LEFT BLANK

APPENDIX C. ADDITIONAL NOTES ON THE NEED FOR STRICT MANUFACTURING CONTROL OVER THE METAMATERIALS

The finite element model of the broadband metamaterials presented in Figure 6 was born out of a vain struggle to build a complete unit cell model that could accurately approximate the experimental prototype metamaterials depicted in Figure 9. The initial attempt involved building the model directly from the specification sheet provided by the manufacturer. The result is shown in Figure 17.

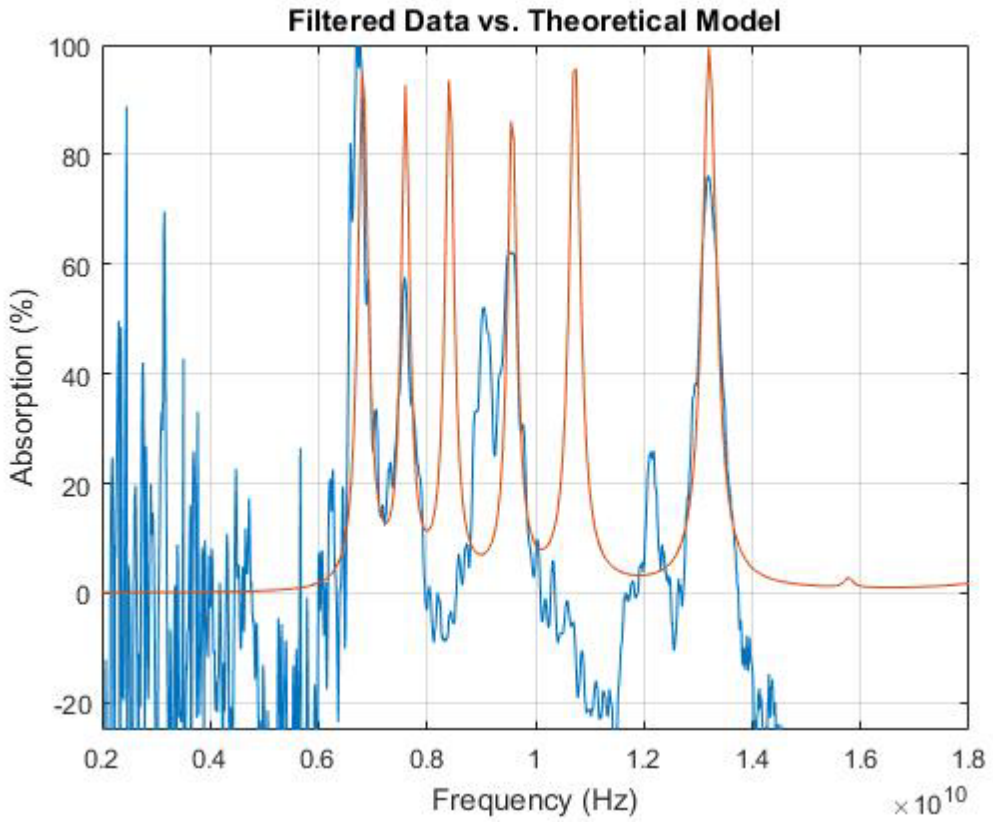

Figure 17. Comparison of Experimental Data and Broadband Model Derived from Manufacturer's Specifications.

As can be seen, two of the absorption peaks are out of place in terms of frequency response. My initial reaction was that the manufacturer had used the

wrong width when installing two of the conductor plates. The SEM micrographs of Figure 10 were actually taken to verify the dimensions of the internal structure of the unit cell. Use of SEM uncovered that the conductor plates were off by as much as 0.1 mm in width, and that the dielectric layers were off by as many as 100 µm in depth. While these discrepancies were significant, when incorporated into the model they did not fully correct the resonant frequency response.

Further investigation ultimately revealed that the manufacturer had used two different grades of fiberglass with completely different permittivity characteristics, and that the difference in permittivity was the source of the discrepancy for the two peaks that were out of place. The 5 mm, 7 mm, 9 mm, and 10 mm plates were all mounted on Prepreg 2116 with a fairly consistent permittivity of 4.4 throughout the analyzed spectrum, resulting in the predictable responses at 6.7 GHz, 7.5 GHz, 9.5 GHz, and 13.4 GHz. On the other hand, the 6 mm and 8 mm plates were mounted on FR4 epoxy, with permittivity ranging between 3.4 and 3.8 across the spectrum, resulting in the two unpredictable responses. The impact of having the wrong resonator widths or dielectric constants can be readily seen with Equation 9. Ultimately the correct permittivity was applied to the model (with a linear regression for FR4) resulting in the comparison in Figure 18.

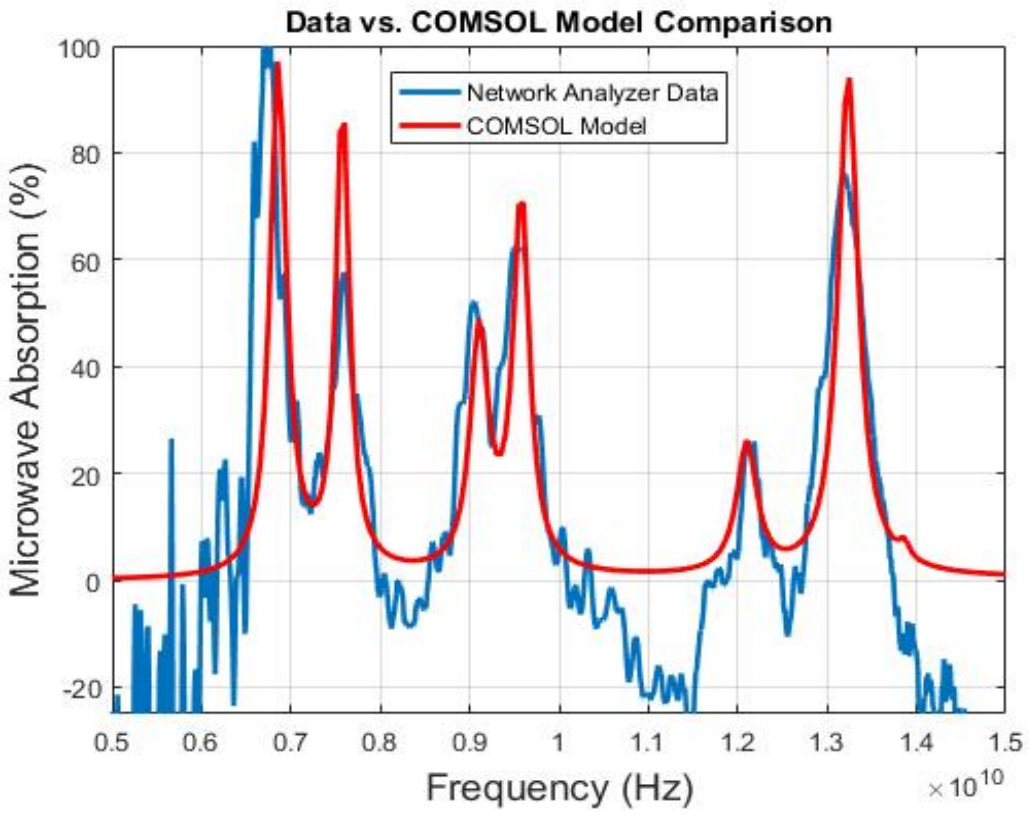

Figure 18. Comparison of Experimental Data and Broadband Model with Corrected Permittivity.

Even though the model is considerably improved, it still runs on what is basically a guess for the dielectric constant of the fiberglass layers. Without accurate dimensions and detailed material properties complete with imaginary components, the complete unit cell is nearly impossible to model accurately.

Although the source of the error was ultimately found, the anecdote stresses the need for tight control over manufacturing tolerances as well as the need for full understanding of the material properties involved. The struggle of generating the complete unit cell model was actually a large motivation in moving toward an algorithm that could generate equivalent medium parameters and a homogenized model that could generate an accurate response with those parameters.

THIS PAGE INTENTIONALLY LEFT BLANK

LIST OF REFERENCES

[1] T. Chen, S. Li, and H. Sun. “Metamaterial application in sensing.” *Sensors*, vol. 12, art. ID 120302742, 2012.

[2] B. Kearney, F. Alves, D. Grbovic, and G. Karunasiri, “Al/SiOx/Al single and multiband metamaterial absorbers for terahertz sensor applications,” *Optical Eng*., vol. 52, no. 1, 2013, art. ID 013801.

[3] Tian Hao, Liu Hai-Tao, and Cheng Hai-Feng. “A thin radar-infrared stealth-compatible structure: Design, fabrication, and characterization.” *Chin. Phys. B*. vol. 23, no. 2, 2014, art. ID 025201.

[4] M. T. McMahan, “Metamaterial absorbers for microwave detection,” M.S. thesis, Phys. Dept., Naval Postgraduate School, Monterey, CA, 2015.

[5] D. Grbovic, “Metamaterials for counter directed energy weapons,” presented at the ONR FY16-17 CDEW Program Review, Arlington, VA, 2017.

[6] D. R. Smith, S. Schultz, P. Markos, and C. M. Soukoulis. “Determination of effective permittivity and permeability of metamaterials from reflection and transmission coefficients.” *Physical Review B.* vol. 65, 2002, art. ID 195104.

[7] S. Arslanagić, T. V. Hansen, N. A. Mortensen, A. H. Gregersen, O. Sigmund, R. W. Ziolkowski, and O. Breinbjerg. “A review of the scattering parameter extraction method with clarification of ambiguity issues in relation to metamaterial homogenization.” *IEEE Antennas and Propagation Magazine*, vol. 55**,** no. 2, pp. 91–106, 2013.

[8] X. Chen, T. Grzegorczyk, B. Wu, J. Pacheco Jr., and J. Kong. “Robust method to retrieve the constitutive effective parameters of metamaterials.” *Physical Review B*, vol. 70, 2004, art. ID 016608.

[9] S. Ramakrishna and T. Grzegorczyk, “Metamaterials and homogenization of composites,” in *Physics and Applications of Negative Refractive Index Materials,* 1st ed. Boca Raton, FL: CRC Press, 2009, ch. 2, pp. 29–75*.*

[10] S. Long. “2-Port parameters,” class notes for ECE145A, Dept. of Elec. and Comp. Eng., University of California at Santa Barbara, Santa Barbara, CA, Rev. 11/07.

[11] C. Volat. “Comparison between the use of surface and volume conductivity to compute potential distribution along an insulator in presence of a think conductive layer.” Presented at the 2013 Electrical Insulation Conference, Ottawa, Ontario, Canada, 2–5 June 2013.

[12] F. Alves, B. Kearney, D. Grbovic, N. V. Lavrik, and G. Karunasiri, “Strong terahertz absorption using SiO_2/Al based metamaterial structures,” App. Phys. Lett. vol. 100, no. 11, 2012, art. ID 111104.

[13] L. Xinwang, L. Hongjun, S. Qibing, and N. Huang, “Ultra-broadband and polarization-insensitive wide-angle terahertz metamaterial absorber,” State Key Laboratory of Transient Optics and Photonics, Xi’an Institute of Optics and Precision Mechanics, Chinese Academy of Science, Xi’an, China, 2015, art. ID 710119.

[14] B. Meyerhoffer, “Photograph of anechoic chamber setup,” Naval Research Laboratory, Washington, DC, 2017.

INITIAL DISTRIBUTION LIST

1. Defense Technical Information Center
   Ft. Belvoir, Virginia

2. Dudley Knox Library
   Naval Postgraduate School
   Monterey, California